Adaptive Uplink Transmit Power Mechanism for Energy Efficiency in Infrared-Based LiFi IoT Networks

Muhammad Asad (14phdmasad@seecs.edu.pk)
National University of Sciences and Technology
Saad Qaisar
National University of Sciences and Technology

Research Article

Keywords: LiFi, IoT networks, energy efficiency, adaptive transmit power, infrared uplink

Posted Date: August 2nd, 2022

DOI: https://doi.org/10.21203/rs.3.rs-1902291/v1

Adaptive Uplink Transmit Power Mechanism for Energy Efficiency in Infrared-Based LiFi IoT Networks

Muhammad Asad[1,2*] and Saad Qaisar[1,3†]

[1*]School of Electrical Engineering and Computer Science, National University of Sciences and Technology, Sector H-12, Islamabad, 44000, ICT, Pakistan.
[2]aeroLiFi GmbH, Wessling, 82234, Bavaria, Germany.
[3]Department of Electrical Engineering, University of Jeddah, Jeddah, 23218, Hejaz, Saudi Arabia.

*Corresponding author(s). E-mail(s): 14phdmasad@seecs.edu.pk;
Contributing authors: saad.qaisar@seecs.edu.pk;
†These authors contributed equally to this work.

Abstract

The continuously increasing number of Wireless Fidelity (WiFi) access points have resulted in increased congestion in already congested indoor networks. In recent years, Light Fidelity (LiFi) has presented itself as upcoming access technology to complement WiFi owing to its vast spectrum, high data rates, and secrecy. Infrared (IR) is widely adopted in the uplink of LiFi-based systems. Due to the limited availability of energy in the Internet of Things (IoT) nodes, energy efficiency is vital. This paper presents a client-based adaptive IR uplink transmit power algorithm to enhance energy efficiency while satisfying the data rate requirement of IoT nodes. With hardware-based experimentation with LZ1 IR-LED and Heidi lens, the need for such an adaptive transmit power mechanism is first demonstrated. Simulation-based evaluation is then performed, showing that the proposed algorithm outperforms random and fixed uplink optical powers in terms of energy efficiency and satisfaction of data rate requirements of IoT nodes. The results clearly show the need for hardware design of IR-based IoT nodes with integrated adaptive uplink transmit power algorithms for LiFi IoT networks.

Keywords: LiFi, IoT networks, energy efficiency, adaptive transmit power, infrared uplink

1 Introduction

Internet of Things (IoT) devices vary in their functionalities, ranging from small sensors to high-end processing devices. Around 25 billion IoT devices are expected to be connected by the year 2025 [1]. Such a massive deployment of IoT devices poses several challenges for Beyond 5G networks, including multiple-access, quality of service, scalability, and reliability [2]. Another critical challenge posed by the limited availability of power on IoT devices is the need for energy-efficient communications.

Wireless Fidelity (WiFi) has been dominantly used as a Radio Access Technology (RAT) in indoor Wireless Area Networks (WANs). However, the WiFi Access Points (APs) are expected to increase to 549 million by 2022, with 80% of mobile traffic occurring indoors [3]. This would

result in massive competition in the already congested and limited frequency spectrum. Consequently, wireless communications in the higher frequency spectrum have been researched. Light Fidelity (LiFi), sometimes also referred to as Visible Light Communication (VLC), has appeared to be the most promising candidate with an enormous 300 THz spectrum and expected data rates of up to 10 Gbps [4]. In addition, LiFi also offers other benefits, including better data security and no Radio Frequency (RF) emissions. The LiFi technology also faces specific challenges like obstructions, blockages, and smaller coverage areas [5]. It is worth mentioning that LiFi aims to complement WiFi and not replace it.

Several potential uplink technologies for LiFi have been considered, including Infrared (IR), VLC, and RF [6]. RF for uplink seems to be the most convenient solution. However, it would further increase the congestion in already congested RF networks. As LiFi is also considered a potential candidate in electromagnetic interference sensitive areas, using RF in uplink would also not be possible in such situations. Using VLC in uplink might not only interfere with the VLC downlink channel but will also cause discomfort to the user's eyes because of visible light traveling upwards [7]. IR has the advantage of being similar in properties to the visible light signal and is in the region invisible to human eyes. The achievable data rates by an IR uplink have already been demonstrated [8]. IR uplink design has been significantly researched in the literature. An omnidirectional transmitter and receiver system has been proposed to improve the quality and robustness of the uplink IR channel [9]. An adaptive beam steering mechanism is proposed to improve uplink performance, enhance received optical signal power, and mitigate channel delay spread [10]. A resource allocation scheme for multi-user systems has also been proposed, coping with inter-symbol interference and inter-user interference by choosing the most suitable Light Emitting Diode (LED) [11].

Energy efficiency has been researched in various hybrid networks, including RF, LiFi, and Power Line Communication (PLC) networks, discussed next in the related work. All of these techniques focus on minimizing energy consumption in the downlink direction at the AP and reducing the overall network's energy consumption. However, energy is more limited at IoT nodes, and hence energy-efficient uplink communications are even more vital. Our previous work proposes a novel client-side technique for energy efficiency in hybrid WiFi and LiFi networks [12]. To the best of the authors' knowledge, extending our previous work, this paper presents a first-of-its-kind adaptive uplink transmit power mechanism to improve energy efficiency in IR-based LiFi IoT networks. Such an energy-efficient mechanism is vital for reducing energy consumption at IoT nodes, thus increasing the lifetime of energy-constrained devices. The proposed mechanism distributively runs on each node, avoiding network scalability issues and the need for excessive network signaling.

1.1 Related Work

Energy efficiency in hybrid access technologies networks, including RF/WiFi, LiFi, and PLC networks, has been researched recently. One of the first studies investigating the benefits of energy efficiency in hybrid RF/VLC networks formulates an energy maximization problem subject to power and data rate constraints [13]. With numerical results, it is shown that VLC enhances energy efficiency in a hybrid RF/VLC system considering various factors such as availability of line of sight, number of LEDs, number of end-devices, and fixed power of VLC APs. An extension to this work includes power allocation algorithms for RF and VLC networks [14]. In another work, an energy efficiency resource allocation problem is formulated for software-defined heterogeneous VLC and RF networks [15]. With simulations, it is shown that the proposed algorithm converges within a few iterations while also increasing throughput at specific power consumption. Another work presents an approach to use a VLC AP when illumination is available and an RF AP when there is no illumination [16]. A power consumption minimization problem formulation is further sub-divided into two sub-problems. The first sub-problem evaluates VLC APs that need to be illuminated, whereas the second sub-problem proposes using an online algorithm to satisfy users' real-time requests. Considering Quality of Service (QoS) requirements from the users present in femtocells, an energy efficiency maximization algorithm is presented [17]. Energy efficiency is

achieved by reducing circuit powers of VLC and RF APs.

The aspects of energy efficiency and spectral efficiency are discussed by introducing VLC in a two-tier RF network [18]. An energy-efficient resource allocation scheme, subdivided into user association and power control, is proposed. Simulation results show that the three-tier network has significantly increased throughput, energy efficiency, and spectral efficiency. In another work, by analyzing dimming control and power constraints, optimal power allocation schemes for hybrid RF/VLC systems with single and multiple LEDs are developed for energy efficiency maximization [19]. Numerical results show that higher gain channels are first assigned power to maximize energy efficiency. The issue of overall power consumption minimization is also considered in hybrid RF/VLC/PLC networks with QoS constraints [20, 21]. A significant improvement in comparison to RF-only networks is shown for such hybrid networks in energy efficiency and throughput.

Power allocation and subchannel allocation optimization problem in VLC systems for energy efficiency is formulated as non-convex problem and then converted to several convex problems [22]. An iterative solution with fast convergence is proposed. Simulation results show that the proposed scheme outperforms conventional schemes in terms of energy efficiency. An energy-efficient Non-Orthogonal Multiple Access (NOMA) technique is presented for multi-user VLC systems [23]. In the proposed multi-access technique, the user QoS is guaranteed by an optimal power allocation strategy to minimize the overall consumed system transmit power, thus maximizing energy efficiency. In another similar work, an adaptive channel and QoS-based user pairing approach is proposed based on channel gain and QoS requirements of the users [24]. Multiple Input Multiple Output (MIMO) is combined with NOMA to provide a high data rate and low error rate downlink system [25]. The proposed system achieves transmitter and receiver diversity by using repetition coding and equal gain combiner. A methodology based on optimal transmitter configuration using lighting constraints is proposed to improve the signal to interference plus noise ratio [26]. The optimal parameters selection at the transmitter are used to obtain an uncorrelated channel, mitigating co-channel interference from neighboring nodes and inter-symbol interference due to multipath reflection.

There has been some recent research interest in using machine learning for hybrid WiFi and LiFi networks. A reinforcement algorithm running on a central controller selects optimal AP for load balancing between WiFi and LiFi networks [27]. An artificial neural network has been used for handover between WiFi and LiFi APs, based on resource availability, mobility, and channel quality [28]. Another work focuses on improving AP selection using two different online learning algorithms based on historical rewards for APs [29]. As the LiFi channel blockage detection is not very accurate at the client-side, Support Vector Machine (SVM) has been used at a central unit to correlate blockages between adjacent periods [30]. All these machine learning approaches are centralized and require much additional processing, as well as learning. Specifically for the expected massive deployment of IoT nodes in Beyond 5G networks, using distributive approaches would avoid network scalability and excessive signaling issues [31]. Therefore, such machine learning-based approaches are not considered for our proposed distributed algorithm.

The related work on the energy efficiency in LiFi networks and the proposed technique is compared in Table 1. The comparison is based on access networks used, network devices considered for energy efficiency, solution method, QoS constraint, and experimental parameters.

1.2 Contribution

The related work shows that the current focus of optimizing energy efficiency in LiFi networks is in the downlink direction at APs. Our previous work presented a first-of-its-kind client-based energy minimization technique for QoS provisioning in hybrid WiFi and LiFi networks [12]. This paper extends our previous work, and presents a novel adaptive uplink transmit power mechanism to optimize energy efficiency distributively at the client-side. The new contributions made by this paper include:

- An IR-based uplink energy efficiency maximization problem is formulated.

Table 1 Comparison of related work on energy efficiency in LiFi networks

Referred Study	Access Network(s)	Energy Efficiency Device(s)	Solution Method	QoS Constraint	Experimental Parameter(s)
[14]	Hybrid RF & LiFi (VLC)	APs	Optimization Theory	Data rate	Number of users, number of LEDs, transmit power, Line of Sight (LoS) availability
[15]	Hybrid RF & LiFi (VLC)	APs	Optimization Theory	Data rate	Number of users, half power semi-angle, size of room, number of LEDs, LoS availability
[16]	Hybrid RF & LiFi (VLC)	APs	Optimization Theory	-	Number of users, data rate requirement
[17]	Hybrid RF & LiFi (VLC)	APs	Optimization Theory	Data rate	Transmit power
[18]	Hybrid RF & LiFi (VLC)	APs	Optimization Theory	Data rate	Number of users, data rate requirement
[19]	Hybrid RF & LiFi (VLC)	APs	Optimization Theory	Data rate	Number of LEDs, data rate requirement, number of RF antennas, transmit power
[20]	Hybrid RF, LiFi (VLC) & PLC	APs	Optimization Theory	Data rate	Transmit power, data rate requirement
[21]	Hybrid RF, LiFi (VLC) & PLC	APs	Optimization Theory	Data rate	Number of users
[22]	LiFi (VLC)	APs	Optimization Theory	Data rate	Number of users, transmit power, sub-channel bandwidth
[23]	LiFi (VLC)	APs	Optimization Theory	Data rate	Number of users, horizontal separation
Proposed Technique	LiFi (IR)	IoT Nodes or Clients	Optimization Theory	Data rate	Number of users, data rate requirement, transmit power, vertical separation

- A novel algorithm for maximizing energy efficiency while considering data rate requirements of IoT nodes is proposed.
- For proof-of-concept, hardware-based experimentation is performed to demonstrate the need for such an adaptive transmit power mechanism.
- With the help of simulations in IR-based LiFi networks, the energy efficiency benefits of the proposed algorithm are demonstrated.

The rest of the paper is organized as follows. The system model and problem formulation are presented in Section 2. Section 3 presents the proposed solution along with the proposed algorithm. Hardware experimentation for proof of concept is presented in Section 4, whereas the simulation results are shown in Section 5. Section 6 concludes the paper.

2 System Model

This section presents the LiFi channel model and formulates the energy efficiency maximization problem.

2.1 LiFi Channel Model

Consider N nodes to be the number of IoT nodes under the coverage of a single LiFi AP, specified by set $\mathcal{N}$. The LiFi IR uplink data rate r_n between the LiFi AP and the n-th node is defined as:

$$r_n = t_n \frac{B}{2} \log_2\left(1 + \frac{e}{2\pi} SNR_n\right). \quad (1)$$

Here, B is the bandwidth assigned by the LiFi AP to an IoT node, t_n is the proportion of time offered by the AP to the node, e is the exponential constant, and SNR_n is the signal-to-noise ratio between the node and the AP. The equation 1 used for calculating data rate is different from Shannon capacity, usually used to calculate data rate in RF networks. This is because of a gap between the Shannon capacity and the actual capacity of a LiFi channel because of the non-negative nature of LiFi signals [32].

A Time Division Multiple Access (TDMA) mechanism is used among the IoT nodes under a single LiFi AP, assuming that no interference occurs between them. It is also assumed that no interference occurs from nodes of neighboring LiFi APs because of physical separation and clock synchronization among multiple LiFi APs. In such a scenario, SNR_n can be given as: [33]

$$SNR_n = \frac{(R_{pd}\ H_n\ P_n\ /\ \kappa)^2}{N_n\ B}. \quad (2)$$

Here, R_{pd} is the responsivity of the photodetector, H_n is the LiFi channel between the AP and the node n, P_n is the optical transmission power at node n, and κ is modulation coefficient for optical to electrical conversion. Whereas, N_n is the Power Spectral Density (PSD) of noise between node n and LiFi AP.

The IR uplink propagation geometry is shown in Figure 1. The angle of irradiance (ϕ) is the angle defined with respect to the perpendicular axis of the IoT node. Whereas the angle of incidence (ψ) is defined with respect to the perpendicular axis of the LiFi AP. Assuming the signal received at uplink by the AP is made up only of the LoS component, H_n can be given as: [33, eq. (1)]

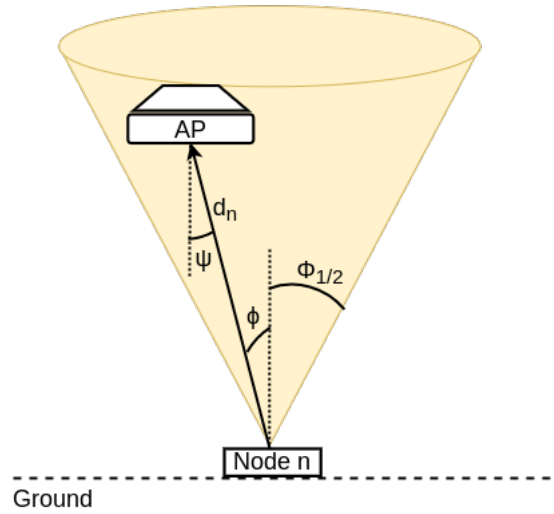

Fig. 1 IR uplink propagation geometry

$$H_n = \frac{(m+1)A_{pd}}{2\pi d_n^2} \cos^m(\phi) g_f g_c(\psi) \cos(\psi). \quad (3)$$

Here, A_{pd} is the physical area of the photodetector at the AP, d_n is the distance between the AP and the node n, and g_f is the optical filter gain. The half-intensity radiation angle, where the intensity of uplink reduces to half of the main beam, is defined by $\Phi_{1/2}$. The Lambertian emission order m is then given as: [33, eq. (2)]

$$m = \frac{-ln(2)}{ln(cos\Phi_{1/2})}. \quad (4)$$

With the semi-angle of field of view given as Ψ_{max}, and f as the refractive index, the optical concentrator gain $g_c(\psi)$ is given as:

$$g_c(\psi) = \begin{cases} \dfrac{f^2}{sin^2(\Psi_{max})} & ,0 \le \psi \le \Psi_{max} \\ 0, & ,\psi > \Psi_{max} \end{cases}. \quad (5)$$

By substituting equation 2 in equation 1:

Table 2 System model descriptions and notations

Description	Notation
Set of IoT Nodes	$\mathcal{N}$
Number of IoT Nodes	N
Uplink data rate of node n	r_n
Bandwidth assigned by LiFi AP to a node	B
Proportion of time offered by AP to node n	t_n
Exponential constant	e
Signal-to-noise ratio between AP and node n	SNR_n
Responsivity of photodetector	R_{pd}
Uplink channel between AP and node n	H_n
Uplink transmit power of node n	P_n
Optical to electrical conversion coefficient	κ
Power Spectral Density (PSD) of noise between AP and node n	N_n
Angle of irradiance	ϕ
Angle of incidence	ψ
Physical area of photodetector	A_{pd}
Distance between AP and node n	d_n
Optical filter gain	g_f
Half-intensity radiation angle	$\Phi_{1/2}$
Lambertian emission order	m
Semi-angle of field of view	Ψ_{max}
Refractive index	f
Optical concentrator gain	g_c

$$r_n = t_n \, \frac{B}{2} \log_2\left(1 + \frac{\mathrm{e}}{2\pi} \frac{(R_{pd} \, H_n \, P_n \, / \, \kappa)^2}{N_n \, B_n}\right). \quad (6)$$

The equation 6 shows that the available data rate r_n at node n is logarithmically proportional to the transmit uplink power P_n. This indicates that although r_n will initially increase significantly with increasing values of P_n, the rate of increase of r_n will keep on decreasing as the value of P_n increases. All the notations used in the channel model are summarized in Table 2.

2.2 Problem Formulation

If Q_n is the power consumed by a node n for its operation and Q_p is the power consumed by the proposed mechanism, the energy efficiency η_n at node n is defined as: [12, eq. (12)]

$$\eta_n = \frac{r_n}{Q_n + Q_p + P_n}. \quad (7)$$

Ignoring the values that will not used for power adaption, Q_n and Q_p, the energy efficiency η_n at node n is defined as:

$$\eta_n = \frac{r_n}{P_n}. \quad (8)$$

Assuming node n has a b_n bits data to transmit, energy efficiency can be improved by optimal selection of transmit data rate and transmit power. We formulate the energy efficiency maximization problem at node n as:

$$max \ (\eta_n), \quad (9)$$

subject to the following constraints:

$$C1 : P_{min} \leq P_n \leq P_{max}. \quad (10)$$

$$C2 : r_n \geq r_{min}. \quad (11)$$

The first constraint C1 ensures that the transmit power P_n at node n stays between P_{min} and P_{max}. Here, P_{min} could be the minimum power required to establish a connection between the AP and the node. On the contrary, P_{max} could either be the maximum transmit power of the node or the maximum power at which the node saturates the receiver at the AP. Another factor limiting P_{max} could be the maximum transmit power that should be safe for human eyes, usually not more than 1W for infrared. The second constraint C2 ensures that the available rate at node r_n should be greater than the minimum required rate r_{min}. Various factors could impact the selection of r_{min}, including the data to transmit b_n, buffer size, application, and use-case requirements. For example, real-time audio communication might require a certain minimum data rate.

There is also a possibility that constraint C2 could not be satisfied when a rate desired by the node could not be provided. Communication could still take place in such a situation. However, constraint C1 should never violate the upper boundary, i.e., the power P_n must never exceed P_{max}.

3 Proposed Solution

Scalability would be a considerable challenge with the massive deployment of IoT devices in Beyond 5G networks. We propose a scalable and distributed mechanism to solve the formulated problem at the client-side without any additional signaling. Such a solution would not introduce additional control traffic as well as no additional load on network-core devices. Only the number of connected clients to an AP is added to the AP's continuously broadcasted information in beacons to all the clients.

The equation 2 defines the SNR for the uplink channel. The same equation could be used for computing the SNR of the downlink channel, whereas the Signal Strength (SS) would only be the numerator of the equation. Modern-day devices know the downlink SS from an AP, SS_{DL}. Using this information, the downlink channel H_{DL} can be computed as:

$$H_{DL} = \frac{\kappa \sqrt{SS_{DL}}}{R_{pd}\ P_{AP}}. \tag{12}$$

Here R_{pd} is the responsivity of the photodetector at the node, and P_{AP} is the transmit power of the LiFi AP. The values of κ, R_{pd} and P_{AP} are constants, and it is assumed that all the IoT nodes already know these values. It is also assumed that the transmitters and receivers are co-located with the same orientation, and the Lambertian emission order and the area of photodetectors are the same. If these assumptions do not hold, the corresponding parameter value has to be transmitted from the AP to the nodes.

As the uplink and downlink channels are nearly similar, the value of H_{DL} could be used as H_n in the uplink channel. With any rate r_n satisfying constraint C2, the corresponding minimum uplink power P_n satisfying constraint C1 can then be computed by using equation 6:

$$P_n = \frac{\kappa}{R_{pd}\ H_n} \sqrt{\left(2^{\frac{2r_n}{t_n B}} - 1\right)\left(\frac{2\pi\ N_n\ B}{\mathrm{e}}\right)}. \tag{13}$$

With the values of r_n, t_n, and H_n known, and an estimated fixed value used for N_n, all other values are constant in equation 13. As the data rate requirement of the node r_n varies over time, the power P_n can be adapted accordingly. For this purpose, an algorithm is proposed next.

3.1 Algorithm

The Algorithm 1 is presented for the proposed adaptive uplink transmission power selection for energy efficiency, and is derived from our earlier proposed algorithm [12]. The algorithm runs distributively at all nodes. At the time t, various parameters are input to the algorithm, as shown in line 1. The output of the algorithm is the calculated adaptive uplink transmit power P_n at time t. Such an Algorithm 1 is considered as a non-cooperative game-theory based distributed algorithm. In such a game, the set of nodes $\mathcal{N}$ is considered as the set of players, and the possible uplink transmit powers can be considered as the set of strategies.

The downlink channel H_{DL} is estimated using equation 12 in line 4. Based on input values of P_{min} and P_{max}, the data rate lower bound r_l and upper bound r_u are calculated using equation 6 in line 5 and line 6, respectively. Line 7 checks to

Algorithm 1 Proposed algorithm

1: Input: $SS_{DL}, R_{pd}, P_{AP}, t_n, B_n, N_n, r_{min}$,
2: b_n, P_{min}, P_{max}
3: Output: P_n
4: **while** true **do**
5: Estimate H_{DL} from equation 12
6: Calculate r_l using P_{min} from equation 6
7: Calculate r_u using P_{max} from equation 6
8: **if** $b_n > 0$ **then**
9: **if** $r_{min} > r_u$ **then**
10: Break; no possible solution exists
11: **else**
12: $r_{temp} = max(r_l, r_{min})$
13: **while** $r_{temp} \leq r_u$ **do**
14: Calculate P_{temp} using r_{temp} from equation 13
15: Calculate η_{temp} using r_{temp} and P_{temp} from equation 8
16: **if** $\eta_{temp} > \eta$ **then**
17: $\eta_n = \eta_{temp}$
18: $P_n = P_{temp}$
19: **end if**
20: $r_{temp} = r_{temp} + \delta$
21: **end while**
22: **end if**
23: **end if**
24: **end while**

calculate P_n only if there is any data in the buffer. If r_{min} is greater than r_u in line 8, the next line 9 breaks while-loop because the constraint C2 is violated. A temporary data rate variable r_{temp} is initialized with maximum value from r_l and r_{min} in line 11.

Different values of r_{temp} are used up to r_u with increments of δ in inner while-loop from line 12 to line 20. For each value of r_{temp}, uplink power P_{temp} and energy efficiency η_{temp} is calculated in line 13 and line 14, respectively. Line 15 checks if energy efficiency is improved. If yes, the η_n and P_n are updated in line 16 and line 17, respectively. At the end of each iteration of the inner while-loop, the transmit power P_n that provides the highest energy efficiency among tested values of r_{temp} is available.

The value of δ used in line 19 could impact the output of the algorithm. For a smaller value, the optimality of the algorithm may improve. However, the number of iterations of the inner while-loop will increase. On the other hand, a higher value of δ may reduce the iterations of the inner while-loop but may also reduce the chances of finding a more optimal solution.

3.2 Complexity and Convergence

The Algorithm 1 has two nested loops. The outer loop is repeated for every time instant. At each time instant, the inner while-loop is repeated $(r_u - r_{temp})/\delta$ times. In Big O notation, the algorithmic complexity at each time instant is linear i.e. $O((r_u - r_{temp})/\delta)$.

The non-cooperative game with the set of nodes $\mathcal{N}$ as the set of players and the possible uplink transmit powers as the set of strategies, is guaranteed to converge to Nash Equilibrium, where each node considers its selection to be optimal given the choices of all other nodes (Theorems 1 - 3, [34]).

4 Proof of Concept: Hardware Experimentation

For the proof of concept, a hardware-based setup shows that although the data rate increases with increasing transmit power until saturation point, the rate of increase in data rate reduces at higher transmit power. This ultimately results in lower energy efficiencies with increasing transmit power. To the best of the authors' knowledge, there is no LiFi equipment available in the market that dynamically adjusts its transmit power. The LiFi APs and clients transmit at constant power. Although, a pureLiFi LiFi-XC generation AP allows to manually adjust the transmit power of the LED in the downlink direction. Using an IR-based LED in downlink direction with LiFi-XC AP and manually adjusting the transmit power, we can argue that similar behavior can be seen in an IR-based uplink direction with an adaptive transmit power mechanism integrated inside the IoT node.

4.1 Setup

A pureLiFi LiFi-XC generation system has an Ethernet-based AP providing a full-duplex data rate of 43 Mbps and a USB-A-based receiver LiFi dongle [35]. By using TDMA, the LiFi-XC system can support eight users simultaneously. Figure 2 shows the hardware experimentation setup. The

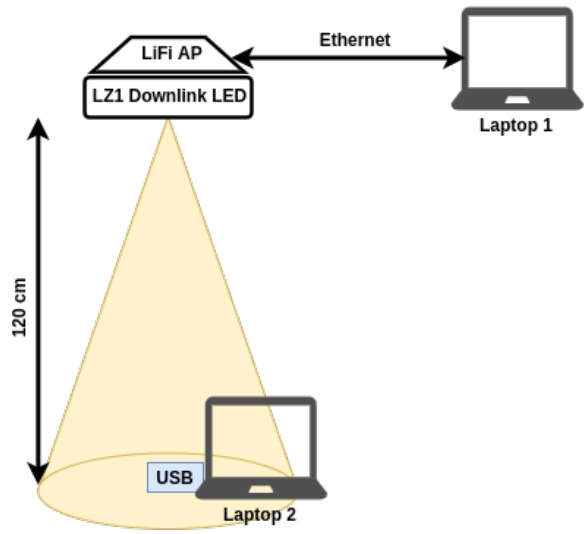

Fig. 2 Hardware experimentation setup

LiFi dongle is inserted in Laptop 2, whereas another Laptop 1, also running DHCP server, is connected with the AP via the Ethernet interface. An LZ1-00R702[1] infrared LED is connected to the AP through the LED driver. In some measurements, Heidi[2] lens is used along with the LED. The vertical separation between LiFi AP and the LiFi dongle is 120 cm, while the angle of incidence and the angle of irradiance are both 0°. The LZ1 LED operates at 940 nm and has an ultra-small footprint of 4.4 mm x 4.4 mm. The Heidi lens has an approximately 50° x 11° oval beam and a dimension of 21.6 mm x 11.7 mm.

The data rate measurement is performed using the iperf utility by running an iperf server on Laptop 1 and an iperf client on Laptop 2. The data rate is measured for a single client in our setup. For multiple clients, the data rate would be distributed among them due to the use of TDMA. Each experiment is repeated ten times for results, with the data-point representing the mean value and the error bar showing the standard deviation.

To evaluate the available data rate and energy efficiency, the LED current is varied. The AP allows for varying the current provided to the LED with an LED driver up to 700 mA. In our experimentation, the current is varied from connection

[1][Online]. Available: https://media.osram.info/media/img/osram-dam-5412883/LED_Engin_Datasheet_LuxiGen_LZ1-00R702_rev2.pdf, accessed in July 2022

[2][Online]. Available: https://www.ledil.com/data/prod/Heidi/12949/12949-ds.pdf, accessed in July 2022

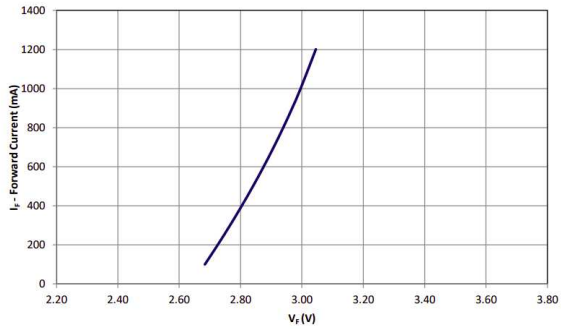

Fig. 3 Typical forward voltage vs forward current characteristics of LZ1 LED

establishment to receiver saturation in steps of 35 mA. The corresponding forward voltage curve for different forward current levels for LZ1 LED is shown in Figure 3[1].

4.2 Results

The data rate measurement results for our hardware experimentation setup are shown in Figure 4. For only LZ1 LED in Figure 4a, the connection is established at 210 mA, with the data rate increasing till 525 mA. As the data rate decreases beyond 525 mA, indicating saturation, the region from 210 mA to 525 mA is considered the operational region. A lens is responsible for concentrating light-emitted by the LED. Therefore, LEDs with the lens are more focused but have a smaller coverage area. The impact of a lens on LED is shown in Figure 4b. As the Heidi lens focuses the beam from the LZ1 LED, the connection establishes at smaller current values of 70 mA and saturates earlier, with data rate decreasing beyond 280 mA. The operational range of LED is considered to be from 70 mA to 280 mA with the lens. Another advantage of using a lens is an improved data rate. For LED only, the measured data rates varied from 3.6 to 16.2 Mbps, whereas for LED with lens, the data rates varied from 13.4 to 29.1 Mbps. Both graphs in Figure 4 also confirm the trend that the data rate initially increases rapidly with increasing current. However, as the current values become higher, the rate of increase of data rate reduces till it becomes stable before going into saturation point.

For energy efficiency comparison, there is a need to map the current to the consumed power. Such a mapping can be performed by using approximate forward voltage values from Figure 3.

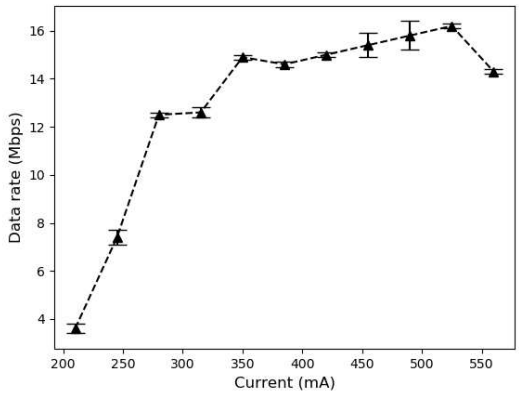

(a) With LZ1 LED

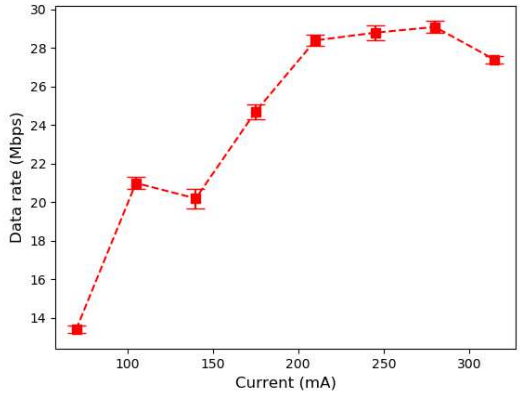

(b) With LZ1 LED and Heidi lens

Fig. 4 Measured data rate by varying LED current

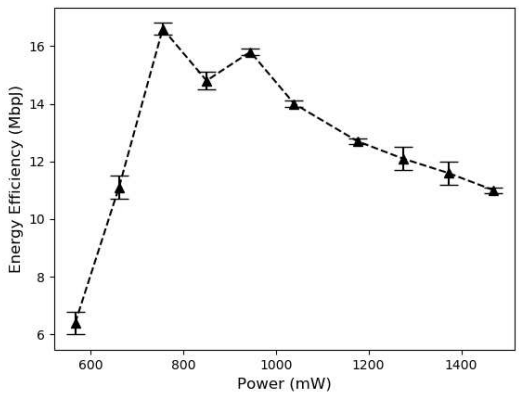

(a) With LZ1 LED

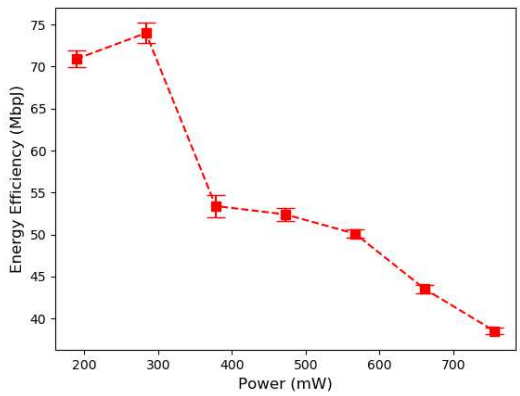

(b) With LZ1 LED and Heidi lens

Fig. 5 Energy efficiency for different transmit powers

The current values in our setup range from 70 mA to 525 mA. We consider the approximate voltage value to be 2.7 V till 385 mA, and 2.8 V till 525 mA. Using this mapping and Figure 4, the energy efficiency is plotted in Figure 5.

The energy efficiency is dependent on the data rate. The energy efficiency increases initially as power increases. However, as the rate of increase of data rate reduces, energy efficiency starts to decrease. As shown for LZ1 LED in Figure 5a, the maximum energy efficiency of 16.6 MbpJ is observed at a transmit power of 756 mW. The data rate available at this point is 12.5 Mbps. Beyond 756 mW, the data rate increases, but energy efficiency continuously decreases. A maximum data rate of 16.2 Mbps is observed at 1470 mW transmit power, but the energy efficiency is just 11 MbpJ. A similar trend can be seen for LZ1 LED with Heidi lens in Figure 5b. However, as higher data rates are achieved by using a lens, the energy efficiency is also significantly higher. In this graph, the energy efficiency increases up to 74 MbpJ till transmit power of 283.5 mW, with an available data rate of 21 Mbps. For a higher data rate requirement, higher transmit powers could be used with 756 mW transmit power providing 29.1 Mbps, but the energy efficiency of only 38.5 MbpJ.

These results indicate that our proposed concept of adaptive uplink transmit power, keeping in mind the required data rate, is highly desirable for energy-efficient transmission as well as the quality of service. Based on the constraint of data rate requirement, the transmit power should be adapted to the value at which energy efficiency can be maximized.

5 Simulation-Based Evaluation

5.1 Setup

A single LiFi AP network is considered for simulation-based evaluation, with the number of nodes varied from two to eight. All the nodes are located in the coverage area of the AP. Both the angle of irradiance and the angle of incidence are selected randomly from 0° to 45° for each node. As IoT nodes that can not only transmit some sensing data but also real-time audio and video are considered, each node requests a random data rate between 5 Mbps and 20 Mbps, corresponding to an average per node data rate of 12.5 Mbps. An example topology with eight nodes, represented by black dots, is shown in Figure 6. For simplicity, the uplink coverage area of only two IoT nodes is shown. All the other nodes would have similar uplink coverage areas.

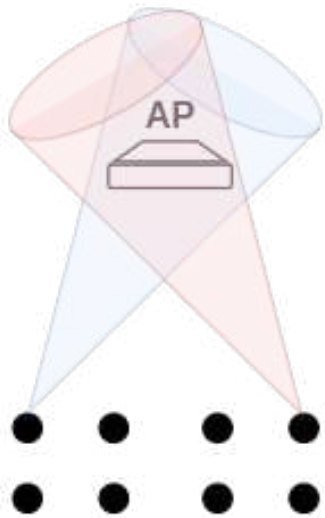

Fig. 6 Simulation setup

Table 3 Simulation parameters

Parameter	Value
LiFi bandwidth, B	20 MHz
Noise PSD, N_n	10^{-21} A^2/Hz
Physical area of photodetector, A_{pd}	10^{-4} m^2
Responsivity of photodetector, R_{pd}	0.53 A/W
Optical filter gain, g_f	1
Refractive index, f	1.5
Optical to electrical conversion coefficient, κ	1
Half-intensity radiation angle, $\Phi_{1/2}$	45°
Photodetector semi-angle of field of view, Ψ_{max}	60°
Angle of irradiance, ϕ	0 - 45°
Angle of incidence, ψ	0 - 45°
Distance between LiFi AP and IoT node, d_n	1 - 2 m
Data rate increment, δ	0.1 Mbps

Our proposed adaptive uplink transmit power algorithm, abbreviated as PA, can transmit at powers ranging from 10 mW to 1000 mW. We compare PA with random and fixed uplink transmit power mechanisms. The random mechanism uses uniform distribution to select transmit power randomly between 100 mW and 1000 mW. Two different fixed uplink transmit powers of 100 mW and 1000 mW are used. The comparison is based on offered data rate, consumed power, energy efficiency, and data rate requirement satisfaction. If the required data rate is provided to the node, it is assumed that the data rate requirement is satisfied. Each data point shown in this section is an average of 10,000 simulation runs, whereas the error-plot represents the standard deviation of these simulation runs. All parameters used for simulation are summarized in Table 3.

5.2 Results

The achieved per node data rate available in the uplink direction for all the schemes are shown in Figure 7. Figure 7a shows the data rate when the distance between the node and AP is 1-meter, and Figure 7b shows the data rate with a 2-meter distance. The data rate is directly related to the signal strength. As the signal strength is inversely proportional to the distance between the nodes and AP, the respective data rate of each scheme is higher for a 1-meter distance compared to a 2-meter distance. For all schemes, the data rate decreases with the increasing number of nodes, as

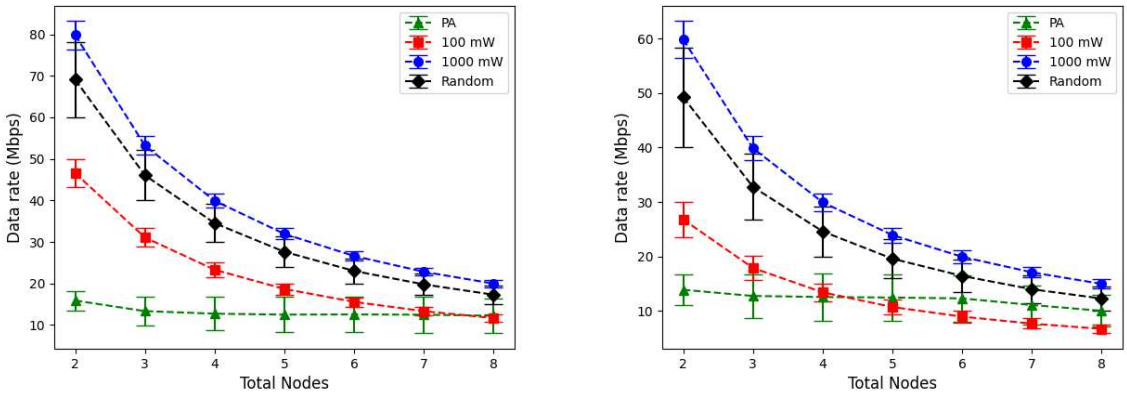

(a) With 1-meter distance (b) With 2-meter distance

Fig. 7 Achieved per node uplink data rate with varying number of nodes

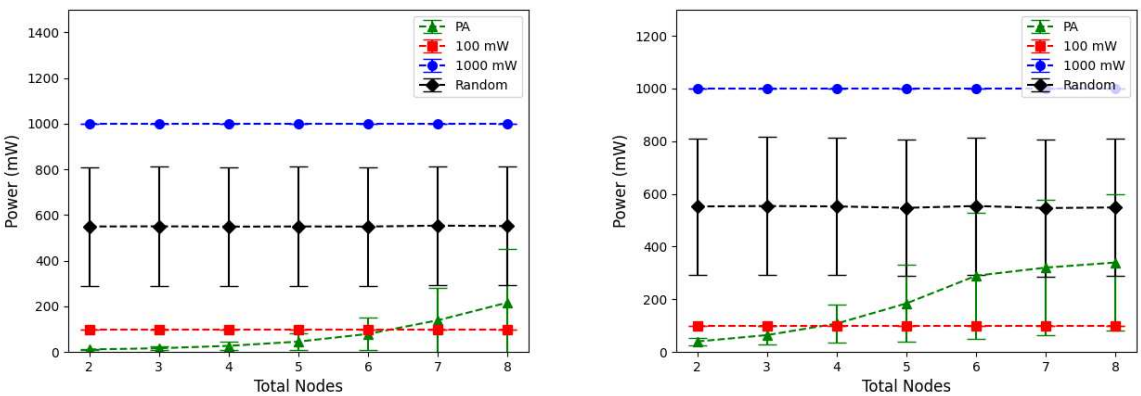

(a) With 1-meter distance (b) With 2-meter distance

Fig. 8 Uplink transmit power with varying number of nodes

the same channel is divided by time slots among a higher number of nodes. For random and fixed power, the data rate continuously decreases with the increasing number of nodes. However, for PA, the decrease in the data rate is not very significant. Due to the integrated mechanism to improve energy efficiency, the PA technique transmits at a data rate optimal for energy efficiency. Although PA could achieve higher data rates similar to 100 mW and 1000 mW techniques, it provides an average per node data rate of 13.09 Mbps at 1-meter and 12.15 Mbps at 2-meter. These data rates are close to the average per-node data rate requirement of 12.5 Mbps.

The uplink transmit power is compared next in Figure 8, with a 1-meter distance between the nodes and the AP in Figure 8a, and a 2-meter distance in Figure 8b. As 100 mW and 1000 mW techniques transmit at constant power, the curve can be seen as a flat-line, irrespective of the number of nodes and distance between the node and the AP. The random technique also has a nearly flat-line because of a large number of simulation repitions. However, the PA adapts the uplink transmit power to optimize energy efficiency. With increasing nodes, the PA increases transmit power to satisfy the nodes' data rate requirement. The transmit power for a 1-meter

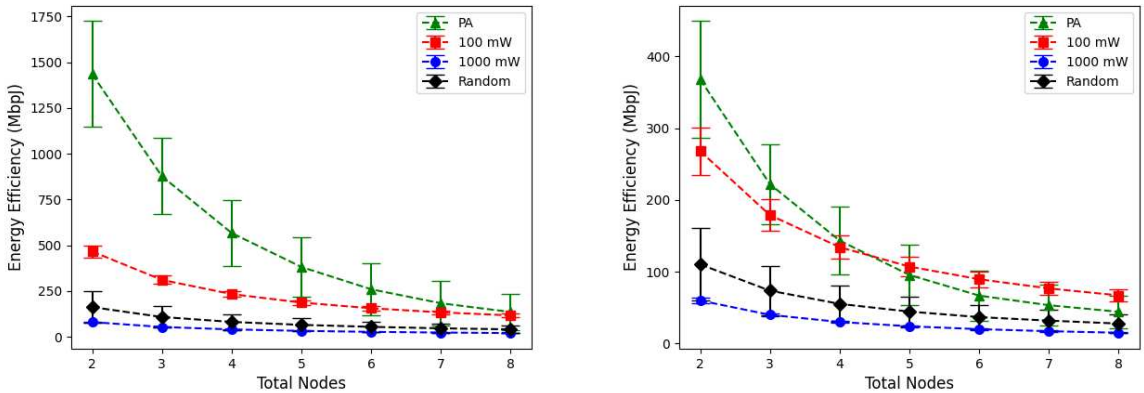

(a) With 1-meter distance

(b) With 2-meter distance

Fig. 9 Energy efficiency with varying number of nodes

distance varies from 11 mW (for two nodes) to 217 mW (for eight nodes), crossing the 100 mW curve for more than six nodes. In comparison, the transmit power varies from 40 mW to 340 mW with a 2-meter distance, crossing the 100 mW curve even earlier at five nodes. However, the transmit power of PA is still significantly lower than random and 1000 mW techniques.

The achieved energy efficiency is compared in Figure 9. As the data rate decreases with the increasing number of nodes for random and fixed uplink power techniques, the energy efficiency also decreases with increasing nodes. For PA, although the data rate does not significantly reduce as the number of nodes increases, the transmit power increases. Therefore, the energy efficiency in PA also decreases with the increasing number of nodes. These trends are also visible in Figure 9. The 1000 mW technique performs the worst, with an average energy efficiency of 39.18 MbpJ at a 1-meter distance and 29.37 MbpJ at a 2-meter distance. The random technique performs better than the 1000 mW technique, having an average energy efficiency of 79.35 MbpJ at a 1-meter distance and 54.23 MbpJ at a 2-meter distance. The PA outperforms the other techniques for a 1-meter distance with an average energy efficiency of 548.26 MbpJ. At 1-meter, the 100 mW technique performs worse than PA but better than random and 1000 mW techniques. The 100 mW technique catches up with PA when the number of nodes becomes eight. However, the average energy efficiency of 228.76 MbpJ of the 100 mW technique is significantly less than PA. For a 2-meter distance, the energy efficiency of the 100 mW technique becomes better than PA as the number of nodes increases beyond four. Still, at a 2-meter distance, the average energy efficiency of 141.84 MbpJ of PA is slightly better than 131.61 MbpJ of the 100 mW technique. It can be assumed that since the PA is designed to improve energy efficiency, it should consistently outperform other techniques for any number of nodes. However, it should be kept in mind that the PA also considers the data rate requirement of the node. If it is possible to satisfy the data rate requirement of the node, the PA will compromise the energy efficiency by increasing the transmit power.

The compromise of energy efficiency to satisfy the data rate requirement of the node can be seen in Figure 10. The percentage of nodes whose data rate requirement is satisfied is shown against the number of nodes. The PA clearly outperforms the random and 100 mW techniques and performs similarly to the 1000 mW technique. This clearly shows that the PA adapts the transmit power as per the data rate requirement of the node. Both PA and 1000 mW techniques almost satisfy the data rate requirement of 100% of nodes for any network size at a 1-meter distance. For 2-meter, both PA and 1000 mW technique completely satisfy data rate requirement till five nodes and then reduces to around 66% by eight nodes. The average data rate satisfaction of PA and 1000 mW technique for 2-meter distance is approximately 92%. On the contrary, the 100 mW technique can

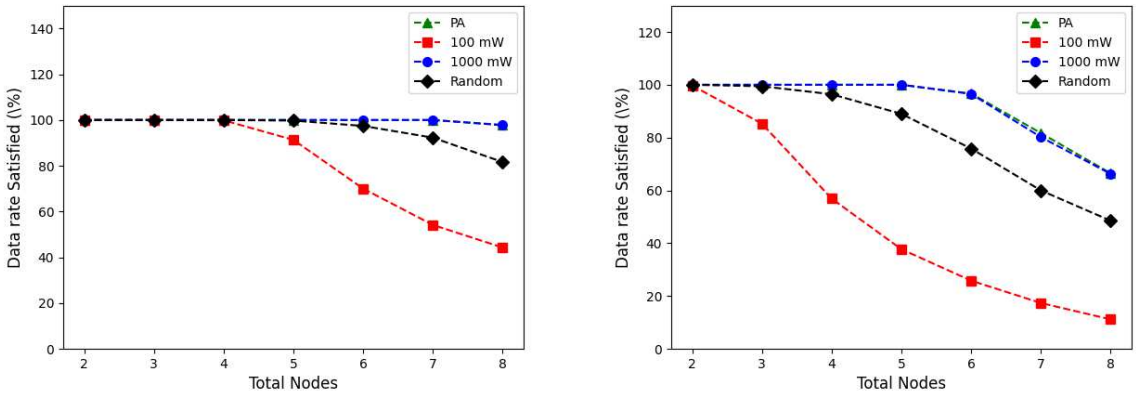

(a) With 1-meter distance

(b) With 2-meter distance

Fig. 10 Percentage of data rate requirement satisfied with varying number of nodes

completely satisfy the data rate requirement until three nodes at 1-meter. The average data rate satisfied by the 100 mW technique is approximately 80% for 1-meter distance and 48% for 2-meter distance. The random technique satisfies the data rate requirement of all nodes till three nodes for 1-meter distance and only a single node for 2-meter distance. On average, the data rate satisfied by random technique is 95.87% for 1-meter distance and 81.31% for 2-meter distance.

5.3 Discussion

For discussion, the energy efficiency results from Figure 9 and data rate satisfied results from Figure 10 have to be seen altogether. The PA and 1000 mW techniques perform similarly and outperform the random and 100 mW techniques for the percentage of data rate satisfied for any number of nodes and for any distance between the AP and the client. However, the energy efficiency of 1000 mW is the worst. The random technique has a slightly better energy efficiency than the 1000 mW but is outperformed by PA and 100 mW techniques. The PA outperforms the 100 mW technique for a 1-meter distance in energy efficiency. Even at 2-meter, the average energy efficiency of PA (141.84 MbpJ) is still slightly better than the 100 mW technique (131.61 MbpJ).

At a 2-meter distance and network size of five or more nodes, the 100 mW technique is slightly more energy efficient than PA. However, the average data rate satisfaction at 2-meter for five or more nodes is approximately 86% for PA and only 23% for 100 mW technique. The slight energy efficiency gain in the 100 mW technique comes with a significant reduction in data rate satisfaction. Considering both energy efficiency and data rate satisfaction, it could be concluded that the PA comfortably outperforms all the other techniques.

6 Conclusion

Due to the expected massive deployment and further congestion of already congested WiFi networks, an adaptive uplink transmit power mechanism is presented in this paper for infrared-based LiFi networks. The proposed algorithm distributively adapts uplink transmit power to optimize energy efficiency at each node while also considering its data rate requirement. The distributed algorithm with linear complexity does not require any additional network component or signaling for its functionality. For proof of concept, hardware-based experimentation with LZ1 LED and Heidi lens shows the need for the proposed algorithm for energy efficiency. Simulation results with a single LiFi AP covering up to eight IoT nodes show that the proposed algorithm provides better energy efficiency and data rate satisfaction when compared with random and fixed uplink transmit powers.

The results demonstrate the potential of the proposed algorithm. With no hardware available in the market to adapt the uplink transmit power for infrared LEDs as per data rate requirement,

this paper clearly shows the need for the hardware development of such a LiFi system.

References

[1] Mourad, A., Yang, R., Lehne, P.H., De La Oliva, A.: A baseline roadmap for advanced wireless research beyond 5g. Electronics **9**(2), 351 (2020)

[2] Asad, M., Basit, A., Qaisar, S., Ali, M.: Beyond 5g: Hybrid end-to-end quality of service provisioning in heterogeneous iot networks. IEEE Access **8**, 192320–192338 (2020)

[3] Forecast, G.M.D.T.: Cisco visual networking index: global mobile data traffic forecast update, 2017–2022. Update **2017**, 2022 (2019)

[4] Zeng, Z., Soltani, M.D., Wang, Y., Wu, X., Haas, H.: Realistic indoor hybrid wifi and ofdma-based lifi networks. IEEE Transactions on Communications **68**(5), 2978–2991 (2020)

[5] Wu, X., Soltani, M.D., Zhou, L., Safari, M., Haas, H.: Hybrid lifi and wifi networks: A survey. IEEE Communications Surveys & Tutorials **23**(2), 1398–1420 (2021)

[6] Pathak, P.H., Feng, X., Hu, P., Mohapatra, P.: Visible light communication, networking, and sensing: A survey, potential and challenges. IEEE communications surveys & tutorials **17**(4), 2047–2077 (2015)

[7] Chen, C., Basnayaka, D.A., Purwita, A.A., Wu, X., Haas, H.: Wireless infrared-based lifi uplink transmission with link blockage and random device orientation. IEEE Transactions on Communications **69**(2), 1175–1188 (2020)

[8] Cossu, G., Wajahat, A., Corsini, R., Ciaramella, E.: 5.6 gbit/s downlink and 1.5 gbit/s uplink optical wireless transmission at indoor distances ($\geq$ 1.5 m). In: 2014 The European Conference on Optical Communication (ECOC), pp. 1–3 (2014). IEEE

[9] Chen, C., Bian, R., Haas, H.: Omnidirectional transmitter and receiver design for wireless infrared uplink transmission in lifi. In: 2018 IEEE International Conference on Communications Workshops (ICC Workshops), pp. 1–6 (2018). IEEE

[10] Alresheedi, M.T., Hussein, A.T., Elmirghani, J.M.: Uplink design in vlc systems with ir sources and beam steering. IET Communications **11**(3), 311–317 (2017)

[11] Selmy, H.A., Elsayed, H.M., Badr, R.I., Eldeeb, H.B., Uysal, M.: Efficient resource allocation scheme in multi-user lifi networks based on angle oriented transceiver. In: 2021 International Conference on Optical Network Design and Modeling (ONDM), pp. 1–3 (2021). IEEE

[12] Asad, M., Qaisar, S.: Energy efficient qos based access point selection in hybrid wifi and lifi iot networks. IEEE Transactions on Green Communications and Networking (2021)

[13] Kashef, M., Ismail, M., Abdallah, M., Qaraqe, K., Serpedin, E.: Power allocation for maximizing energy efficiency of mixed rf/vlc wireless networks. In: 2015 23rd European Signal Processing Conference (EUSIPCO), pp. 1441–1445 (2015). IEEE

[14] Kashef, M., Ismail, M., Abdallah, M., Qaraqe, K.A., Serpedin, E.: Energy efficient resource allocation for mixed rf/vlc heterogeneous wireless networks. IEEE Journal on Selected Areas in Communications **34**(4), 883–893 (2016)

[15] Zhang, H., Liu, N., Long, K., Cheng, J., Leung, V.C., Hanzo, L.: Energy efficient subchannel and power allocation for software-defined heterogeneous vlc and rf networks. IEEE Journal on Selected Areas in Communications **36**(3), 658–670 (2018)

[16] Khreishah, A., Shao, S., Gharaibeh, A., Ayyash, M., Elgala, H., Ansari, N.: A hybrid rf-vlc system for energy efficient wireless access. IEEE Transactions on Green Communications and Networking **2**(4), 932–944 (2018)

[17] Hsiao, Y.C., Chen, C.M., Lin, C.: Energy efficiency maximization in multi-user miso mixed rf/vlc heterogeneous cellular networks. In: 2018 15th Annual IEEE International Conference on Sensing, Communication, and Networking (SECON), pp. 1–9 (2018). IEEE

[18] Aboagye, S., Ibrahim, A., Ngatched, T.M.N., Dobre, O.A.: Vlc in future heterogeneous networks: Energy– and spectral–efficiency optimization. In: ICC 2020 - 2020 IEEE International Conference on Communications (ICC), pp. 1–7 (2020). https://doi.org/10.1109/ICC40277.2020.9148909

[19] Ma, S., Zhang, F., Li, H., Zhou, F., Alouini, M.-S., Li, S.: Aggregated vlc-rf systems: Achievable rates, optimal power allocation, and energy efficiency. IEEE Transactions on Wireless Communications **19**(11), 7265–7278 (2020)

[20] Kashef, M., Abdallah, M., Al-Dhahir, N.: Transmit power optimization for a hybrid plc/vlc/rf communication system. IEEE Transactions on Green Communications and Networking **2**(1), 234–245 (2017)

[21] Aboagye, S., Ibrahim, A., Ngatched, T.M., Ndjiongue, A.R., Dobre, O.A.: Design of energy efficient hybrid vlc/rf/plc communication system for indoor networks. IEEE Wireless Communications Letters **9**(2), 143–147 (2019)

[22] Aboagye, S., Ngatched, T.M., Dobre, O.A., Armada, A.G.: Energy efficient subchannel and power allocation in cooperative vlc systems. IEEE Communications Letters **25**(6), 1935–1939 (2021)

[23] Chen, C., Fu, S., Jian, X., Liu, M., Deng, X.: Energy-efficient noma with qos-guaranteed power allocation for multi-user vlc. In: IEEE Conference on Industrial Electronics and Applications (ICIEA 2021) (2021). IEEE

[24] Chen, C., Fu, S., Jian, X., Liu, M., Deng, X., Ding, Z.: Noma for energy-efficient lifi-enabled bidirectional iot communication. IEEE Transactions on Communications **69**(3), 1693–1706 (2021)

[25] Dixit, V., Kumar, A.: Ber performance of mimo based noma-vlc system with imperfect sic. Transactions on Emerging Telecommunications Technologies, 4422 (2021)

[26] Chatterjee, S., Sabui, D., Khan, G.S., Roy, B.: Signal to interference plus noise ratio improvement of a multi-cell indoor visible light communication system through optimal parameter selection complying lighting constraints. Transactions on Emerging Telecommunications Technologies **32**(10), 4291 (2021)

[27] Ahmad, R., Soltani, M.D., Safari, M., Srivastava, A., Das, A.: Reinforcement learning based load balancing for hybrid lifi wifi networks. IEEE Access **8**, 132273–132284 (2020)

[28] Wu, X., O'Brien, D.C.: A novel machine learning-based handover scheme for hybrid lifi and wifi networks. In: 2020 IEEE Globecom Workshops (GC Wkshps, pp. 1–5 (2020). IEEE

[29] Wang, J., Jiang, C., Zhang, H., Zhang, X., Leung, V.C., Hanzo, L.: Learning-aided network association for hybrid indoor lifi-wifi systems. IEEE Transactions on Vehicular Technology **67**(4), 3561–3574 (2017)

[30] Ji, K., Mao, T., Chen, J., Dong, Y., Wang, Z.: Svm-based network access type decision in hybrid lifi and wifi networks. In: 2019 IEEE 90th Vehicular Technology Conference (VTC2019-Fall), pp. 1–5 (2019). IEEE dsdasds

[31] Asad, M., Qaisar, S., Basit, A.: Client-centric access device selection for heterogeneous qos requirements in beyond 5g iot networks. IEEE Access **8**, 219820–219836 (2020)

[32] Wang, J.-B., Hu, Q.-S., Wang, J., Chen, M., Wang, J.-Y.: Tight bounds on channel capacity for dimmable visible light communications. Journal of Lightwave Technology **31**(23), 3771–3779 (2013)

[33] Wu, X., Safari, M., Haas, H.: Access point

selection for hybrid li-fi and wi-fi networks. IEEE Transactions on Communications **65**(12), 5375–5385 (2017)

[34] Aryafar, E., Keshavarz-Haddad, A., Wang, M., Chiang, M.: Rat selection games in hetnets. In: 2013 Proceedings IEEE INFOCOM, pp. 998–1006 (2013). IEEE

[35] Albraheem, L.I., Alhudaithy, L.H., Aljaser, A.A., Aldhafian, M.R., Bahliwah, G.M.: Toward designing a li-fi-based hierarchical iot architecture. IEEE Access **6**, 40811–40825 (2018)

Author Biography

Muhammad Asad completed his bachelor's in Telecommunication Engineering from the University of Engineering and Technology Taxila, Pakistan, in 2011. He received his master's degree in Communications Engineering from the Technical University of Munich, Germany, in 2013, and Ph.D. in Electrical Engineering from the School of Electrical Engineering and Computer Science (SEECS), National University of Sciences and Technology (NUST), Pakistan, in 2021. He is currently working as System Development Engineer at aeroLiFi GmbH, Germany. His research interests include software-defined networking, quality of service, and IoT networks.

Saad Qaisar received the master's and Ph.D. degrees in electrical engineering from Michigan State University, USA, in 2005 and 2009, respectively. He is currently serving as an Assistant Professor with the School of Electrical Engineering Computer Science (SEECS), National University of Sciences and Technology (NUST), Pakistan. He is the lead researcher and the founding director of the CoNNekT Lab: Research Laboratory of Communications, Networks and Multimedia, National University of Sciences and Technology (NUST), Pakistan. He has published over 80 articles at reputed international venues with a vast amount of work in the pipeline.